

# Clinical Outcomes of Corneal Vertex Versus Central Pupil References with Aberration-Free Ablation Strategies and LASIK

Maria Clara Arbelaez,<sup>1</sup> Camila Vidal,<sup>1</sup> and Samuel Arba-Mosquera<sup>2</sup>

**PURPOSE.** To compare the clinical outcomes of aberration-free ablation profiles based on the normal corneal vertex (CV) and the pupil center (PC) in relation to laser in situ keratomileusis. Aberration-free aspheric ablation treatments were performed in all cases.

**METHODS.** Two myopic astigmatism groups (CV centered using the offset between pupil center and normal corneal vertex and PC centered using the pupil center) comprising 24 and 29 eyes (16 and 19 patients), respectively, with a 6-month follow-up, were included. All enrolled eyes had  $<0.65 \mu\text{m}$  RMS-higher order aberration (HOA) for 6.00 mm analysis diameter and pupillary offset  $>200 \mu\text{m}$ . In all cases, standard examinations, and preoperative and postoperative wavefront analysis were performed. Custom ablation software was used to plan aberration-free aspheric treatments and a flying spot excimer laser system was used to perform ablations. The clinical outcomes were evaluated for predictability, refractive outcome, safety, ocular wavefront aberration, and asphericity.

**RESULTS.** Of the CV eyes, 38% had improved best spectacle-corrected visual acuity (BSCVA) compared with 24% of the PC eyes (comparison CV/PC  $P = 0.38$ ). Induced ocular coma was on average  $0.17 \mu\text{m}$  in the CV group and  $0.26 \mu\text{m}$  in the PC group (comparison CV/PC  $P = 0.01$  favoring CV). Induced ocular spherical aberration was on average  $+0.01 \mu\text{m}$  in the CV group and  $+0.07 \mu\text{m}$  in the PC group (comparison CV/PC  $P = 0.05$  favoring CV). Change in asphericity was on average  $+0.56$  in the CV group and  $+0.76$  in the PC group (comparison CV/PC  $P = 0.05$  favoring CV). No significant shift was observed in the pupillary offset after treatments.

**CONCLUSIONS.** In myopic eyes with moderate to large pupillary offset, CV-centered treatments performed better in terms of induced ocular aberrations and asphericity, but both centration were identical in photopic visual acuity. (*Invest Ophthalmol Vis Sci.* 2008;49:5287-5294) DOI:10.1167/iovs.08-2176

Controversy remains regarding where to center corneal refractive procedures to maximize visual outcomes. A misplaced refractive ablation may result in undercorrection and other undesirable side effects. Pande and Hillman<sup>1</sup> postulated that the coaxial light reflex lies nearer to the corneal intercept of the visual axis than the pupil center (PC) and recommended

that the corneal coaxial light reflex be centered during refractive surgery. Boxer Wachler et al.<sup>2</sup> identified the coaxial light reflex and used it as the center of the ablation. de Ortueta and Arba Mosquera<sup>3</sup> used the corneal vertex (CV) measured by videokeratoscopy as the morphologic reference to center corneal refractive procedures. However, Uozato and Guyton<sup>4</sup> recommended the pupil center as the reference for refractive surgery. Mandell<sup>5</sup> proposed the line of sight as the reference, because it minimizes the required optical zone.

An excimer laser is typically used to alter the corneal curvature and compensate for ocular refractive errors in corneal refractive surgery.<sup>6</sup> This is currently the most successful technique, mainly due to its submicrometer precision and capacity to achieve highly repeatable corneal ablations with minimal side effects. Although standard ablation profiles to correct myopic astigmatism based on removing convex-concave tissue lenticles with spherocylindrical surfaces effectively compensate for primary refractive errors, the quality of vision deteriorates substantially, especially under mesopic and low-contrast conditions.<sup>7</sup> Preoperative wavefront analyses (either corneal or ocular) have created individualized ablation patterns to compensate for preexisting HOAs.<sup>8</sup> Topographic-guided,<sup>9</sup> wavefront-driven,<sup>10</sup> wavefront-optimized,<sup>11</sup> asphericity preserving, and Q-factor profiles<sup>12</sup> have all been proposed as solutions. Parallel to the improvements in more detailed ablation patterns and more capable laser systems, a highly precise and optimal definition of a centration reference is necessary.

In the present study, we compared the postoperative outcomes among eyes treated with laser in situ keratomileusis (LASIK), by using CV or PC as a reference for aberration-free profiles. We evaluated the efficacy, predictability, stability, refractive outcome, and safety of each of the references implemented in the Custom Ablation Manager (CAM; Schwind Eye-Tech-Solutions, Kleinostheim, Germany) software platform and evaluated the impact on HOAs and asphericity.

## MATERIALS AND METHODS

Thirty-five patients (53 eyes) seeking laser correction at the Muscat Eye Laser Center, Sultanate of Oman, were enrolled. Informed consent was obtained from each patient in adherence to the tenets of the Declaration of Helsinki. The patients were divided into two myopic astigmatism groups. In the CV group (24 eyes, 16 patients, 8 patients with both eyes enrolled in the study and 8 patients with one eye enrolled), the ablation was centered by using the pupillary offset (i.e., the distance between the pupil center and the normal CV measured by videokeratoscopy (Keratron Scout topographer; Optikon 2000, SPA, Rome, Italy). The measurement was performed under photopic conditions of 1500 lux, similar to the conditions under the operating microscope according to a method was suggested and described by de Ortueta and Arba Mosquera.<sup>3</sup> The excimer laser allows for modification of the ablation centration from the pupillary center with an offset by entering either  $X$  and  $Y$  cartesian values or  $R$  and  $\theta$  polar values in a regular treatment. The measurement of the pupillary offset was translated into the treatment planning as polar coordinates to be manually entered in the excimer laser computer.

From the <sup>1</sup>Muscat Eye Laser Center, Muscat, Sultanate of Oman; and <sup>2</sup>Schwind Eye-Tech-Solutions, Kleinostheim, Germany.

Submitted for publication April 16, 2008; revised May 30 and June 23, 2008; accepted September 22, 2008.

Disclosure: M.C. Arbelaez, Schwind Eye-Tech-Solutions (R); C. Vidal, None; S. Arba-Mosquera, Schwind Eye-Tech-Solutions (E)

The publication costs of this article were defrayed in part by page charge payment. This article must therefore be marked "advertisement" in accordance with 18 U.S.C. §1734 solely to indicate this fact.

Corresponding author: Maria Clara Arbelaez, Muscat Eye Laser Center, P.O. Box 938; P.C. 117, Muscat, Sultanate of Oman; drmaria@omantel.net.om.

TABLE 1. Preoperative Refractive Data from the Treatment Groups

	CV Group		PC Group	
	Mean $\pm$ SD	Range	Mean $\pm$ SD	Range
Defocus (D)	$-3.14 \pm 1.71$	-6.88 to -0.38	$-3.79 \pm 2.36$	-8.50 to -0.38
Astigmatism (D)	$0.68 \pm 0.73$	0.00 to 2.25	$1.00 \pm 0.94$	0.00 to 4.00
BSCVA	$1.18 \pm 0.23$	0.7 to 1.3	$1.16 \pm 0.20$	0.7 to 1.3
Ocular coma ( $\mu\text{m}$ ) (6.0 mm)	$0.20 \pm 0.09$	0.07 to 0.43	$0.23 \pm 0.10$	0.08 to 0.46
Ocular trefoil ( $\mu\text{m}$ ) (6.0 mm)	$0.15 \pm 0.12$	0.03 to 0.52	$0.17 \pm 0.08$	0.03 to 0.33
Spherical ocular aberration ( $\mu\text{m}$ ) (6.0 mm)	$+0.08 \pm 0.12$	-0.21 to +0.32	$+0.07 \pm 0.18$	-0.31 to +0.42
RMS HOA ( $\mu\text{m}$ ) (6.0 mm)	$0.37 \pm 0.10$	0.21 to 0.58	$0.40 \pm 0.11$	0.24 to 0.66
Pupillary offset (mm)	$0.27 \pm 0.08$	0.20 to 0.52	$0.32 \pm 0.15$	0.20 to 0.85

RMS, root mean square.

In the PC group (29 eyes, 19 patients, 10 patients with both eyes enrolled in the study and 9 patients with one eye enrolled), the ablation was centered by using the pupil center as observed by the eye-tracking module.

### Treatment Selection Criteria

The aberration-free aspherical treatments<sup>11</sup> were used for all treatments. The CAM aspherical profiles were developed to achieve profiles "neutral for aberration" that induce no change in wavefront aberration within the optical zone other than the sphere and cylinder components, leaving all existing HOAs unchanged whenever the BCVA was unaffected by the preexisting aberrations.<sup>13,14</sup> Thus, to compensate for the aberrations induced with other types of profile definitions,<sup>15</sup> some of the sources of aberrations are related to the loss of efficiency of the laser ablation for non-normal incidence.<sup>16,17</sup>

The CAM aberration-free profiles include aspheric profiles to balance the induction of spherical aberration (proliteness optimization) by controlling the postoperative corneal asphericity. The software provides K-reading compensation, which considers the change in spot geometry and reflection losses of ablation efficiency. Real ablative spot shape (volume) is considered through a self-constructing algorithm. In addition, there is a randomized flying-spot ablation pattern that eliminates the risk of thermal damage.

Eyes were enrolled in the study groups only if they had no symptomatic aberrations ( $<0.65 \mu\text{m}$  root mean square (RMS)-HOA (measured by the Schwind Ocular Wavefront Analyzer and the Optikon Keratron Scout for 6.00 mm analysis diameter;  $<0.50 \text{ DEq}^{18}$ ) and moderate-to-large pupillary offset ( $>200 \mu\text{m}$ ). Patients were randomly assigned to the CV or PC centration groups based on a coin toss. In the patients with only one eye fulfilling the enrolling criteria, both eyes were treated with the randomly assigned centration method, but only one eye was included for analysis.

The exclusion criteria included unstable refraction during the previous 6 months; signs of keratoconus or abnormal corneal topography; collagen vascular, autoimmune, or immunodeficiency diseases; severe local infective or allergic conditions; severe dry eye disease; monocularly or severe amblyopia; or cataracts.

To determine the ablation profile of the CAM, the manifest refraction was measured in each eye and cross checked with the objective refraction from the Schwind Ocular Wavefront Analyzer.<sup>19</sup> Preoperative topography and aberrometry measurements were taken, and the VA and mesopic pupil size (Schwind Ocular Wavefront Analyzer) were measured. The ablation for each eye was planned based on the manifest refraction using the CAM aberration-free treatments. In both groups, we used an optical zone of 6.50 mm with a variable transition zone provided automatically by the software in relation to the planned refraction.

In all cases, one surgeon (MCA) performed all standard LASIK procedures at the Muscat Eye Laser Center. Immediately before the ablation, the laser was calibrated according to the manufacturer's

instructions and the calibration settings were recorded. Each eye underwent LASIK, each flap was cut with a superior hinge made by a Carriazo-Pendular microkeratome<sup>20</sup> with a 130- $\mu\text{m}$  head, and each ablation was performed the ESIRIS laser (Schwind).<sup>21</sup> The ESIRIS laser system has a repetition rate of 200 Hz, produces a spot size of 0.8 mm<sup>22,23</sup> (full width at half maximum) with a para-Gaussian ablative spot profile, and controls the local repetition rates to minimize the thermal load.<sup>24</sup> High-speed eye tracking with a 330-Hz acquisition rate is accomplished with a 5-ms latency period.<sup>25</sup>

The manifest refraction, VA, topography, and aberrometry measurements were recorded for each eye at 1, 3, and 6 months and 1 year after surgery.

At the preoperative stage, as well as, at any of the follow-ups after the treatments, the pupillary offset was measured directly at the topographical map displayed by the videokeratoscope, and corresponds to the distance between the pupil center under photopic conditions of 1500 lux and the normal CV.

Optical errors centered on the line of sight, representing the ocular wavefront aberration, were described by the Zernike polynomials<sup>26</sup> and the coefficients of the Optical Society of America (OSA) standard<sup>27</sup> and analyzed for a standardized diameter of 6 mm.

In particular, we analyzed the possible correlations between induced ocular aberrations with defocus correction and with pupillary offset.

As the used profiles are aspherically based aiming for effects neutral for aberration, correlations between induced ocular spherical aberration and defocus assess how close (or how far) the profiles are from the targeted neutral effect when centered according to the different references, whereas correlations between induced ocular coma aberration and defocus assess whether the profiles have a systematic decentration (a spherical aberration analyzed off-axis results in coma aberration) when referred according to different points.

We performed 53 treatments without adverse events using ESIRIS aberration-free aspheric profiles and a 6.5-mm optical zone. Each eye was evaluated at a 6-month follow-up session. Table 1 shows the mean refractive data of the groups.

For statistical analysis, paired *t*-tests were used to compare postoperative versus preoperative results within each group, and unpaired *t*-tests were used to compare results between groups. For correlation tests, the coefficient of determination ( $r^2$ ) was used, and the significance of the correlations was evaluated using probabilities calculated considering a metric distributed approximately as *t* with  $n - 2$  degrees of freedom where *n* is the size of the sample. For all tests,  $P < 0.05$  was considered statistically significant.

## RESULTS

Regarding efficacy, 88% of the eyes in which the treatment was centered on the CV achieved better than 20/20 uncorrected visual acuity 6 months after surgery, compared with 97% of the

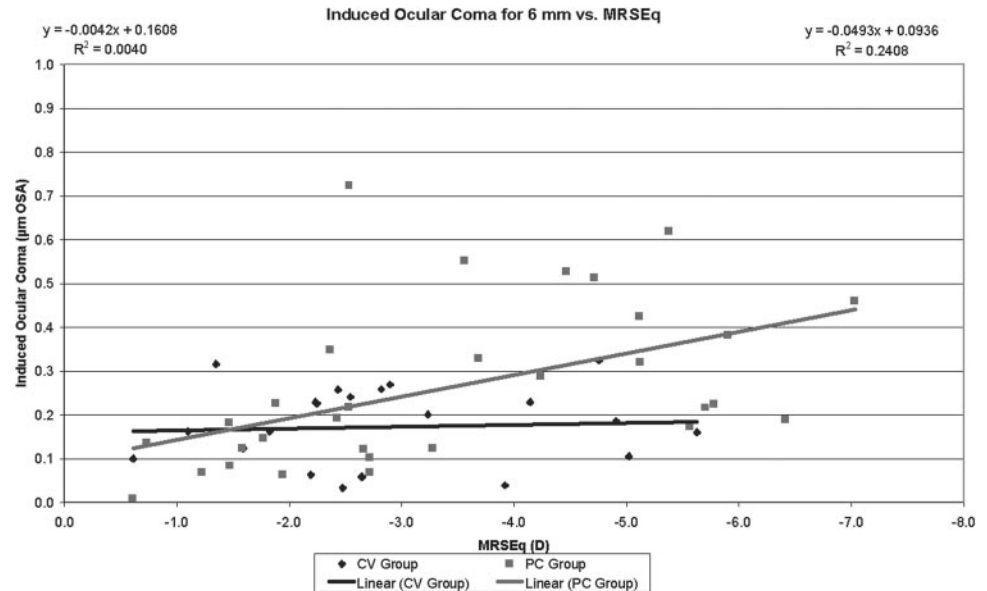


FIGURE 1. Induced ocular coma/diometer focus diopter ratio in the CV and the PC groups.

eyes centered on the PC. However, the difference in efficacy between groups did not reach significance (unpaired *t*-test  $P = 0.25$ ).

Based on the refractive power change (in terms of achieved correction), the sphere and cylinder corrections were accurate, predictable, and stable from the 1-month follow-up.

Regarding refractive outcome, 58% of the eyes centered on the CV were within  $\pm 0.25$  D and 88% were within  $\pm 0.50$  D of the intended corrections 6 months after surgery, whereas 48% of the eyes centered on the PC were within  $\pm 0.25$  D and 83% were within  $\pm 0.50$  D of the intended correction. However, the difference in refractive outcome between the groups was not significant (unpaired *t*-test  $P = 0.10$ ).

Regarding safety, 38% of the eyes centered on the CV had improved BSCVA compared with 24% of the eyes centered on the PC. The improvement in safety was significant in the CV group (paired *t*-test  $P = 0.02$ ) but not in the PC group (paired *t*-test  $P = 0.07$ ). However, the difference in safety between the groups favoring the CV strategy was not significant (unpaired *t*-test  $P = 0.38$ ).

The amount of induced ocular coma was small with both centration strategies: an average  $0.17 \mu\text{m}$  (range,  $0.03$ – $0.32 \mu\text{m}$ ) in the CV group and  $0.26 \mu\text{m}$  (range,  $0.01$ – $0.72 \mu\text{m}$ ) in the PC group. The difference in induced ocular coma between groups favoring CV was significant (unpaired *t*-test  $P = 0.01$ ). Furthermore, the induced ocular coma did not correlate with achieved defocus correction of the eyes treated with the CV strategy ( $r^2 = 0.004$ ,  $P = 0.78$  in the CV group), but it did correlate with achieved defocus correction of the eyes treated with the PC strategy ( $r^2 = 0.24$ ,  $P = 0.01$  in the PC group). The induced ocular coma/diopters of the achieved defocus correction ratio (the slope of the regression) was  $-0.004 \mu\text{m}$  of induced ocular coma/diopters in the CV group and  $-0.049 \mu\text{m}$  of induced ocular coma/diopters in the PC group (Fig. 1).

Theoretically, ocular coma induction is correlated directly with the amount of diopters corrected and the amount of decentration.<sup>28</sup> We analyzed the correlation between the induced ocular coma/diometer focus with the pupillary offset in both groups. No correlation was found for any eyes treated with either centration strategy ( $r^2 = 0.07$ ,  $P = 0.62$  in the CV group;  $r^2 = 0.01$ ,  $P = 0.87$  in the PC group). The difference between groups was not significant (unpaired *t*-test  $P = 0.43$ ).

The induced ocular trefoil was small with both centration strategies (i.e., an average  $0.09 \mu\text{m}$ ; range,  $0.01$ – $0.34 \mu\text{m}$ ) in the CV group and  $0.13 \mu\text{m}$  (range,  $0.01$ – $0.49 \mu\text{m}$ ) in the PC group. The difference in induced ocular trefoil between groups favoring the CV strategy was not significant (unpaired *t*-test  $P = 0.07$ ). Further, the induced ocular trefoil was not correlated with either centration strategy ( $r^2 = 0.01$ ,  $P = 0.69$  for CV group,  $r^2 = 0.11$ ,  $P = 0.07$  in the PC group). The induced ocular trefoil/diopters of achieved defocus correction ratio (the slope of the regression) was  $-0.005$  induced ocular trefoil/diopters in the CV group, and  $-0.019$  induced ocular trefoil/diopters in the PC group (Fig. 2).

The induced ocular spherical aberration was minute with both centration strategies: an average  $+0.01 \mu\text{m}$  (range,  $-0.25$  to  $+0.34 \mu\text{m}$ ) in the CV group and  $+0.07 \mu\text{m}$  (range,  $-0.01$  to  $+0.46 \mu\text{m}$ ) in the PC group. The difference in induced ocular coma between groups favoring the CV strategy was significant (unpaired *t*-test  $P = 0.05$ ). Further, the induced ocular spherical aberration did not correlate with achieved defocus correction in the eyes treated with the CV strategy ( $r^2 = 0.13$ ,  $P = 0.09$  in the CV group), but it did correlate with the achieved defocus correction in the eyes treated with the PC strategy ( $r^2 = 0.17$ ,  $P = 0.02$  in the PC group). The induced ocular spherical aberration/diopters of the achieved defocus correction ratio (the slope of the regression) was  $-0.028 \mu\text{m}$  of induced ocular spherical aberration/diopters in the CV group and  $-0.035 \mu\text{m}$  of induced ocular spherical aberration/diopters in the PC group (Fig. 3).

The change in asphericity was moderate with both centration strategies (i.e., an average  $+0.56$  [range,  $+0.07$  to  $+1.31$ ] in the CV group and  $+0.76$  [range,  $-0.12$  to  $+1.79$ ] in the PC group). The difference in change in asphericity between groups favoring the CV strategy was significant (unpaired *t*-test  $P = 0.05$ ). Further, the change in asphericity correlated with the achieved defocus correction in the eyes treated with both centration strategies ( $r^2 = 0.62$ ,  $P = 0.02$  in the CV group;  $r^2 = 0.18$ ,  $P = 0.04$  in the PC group). The change in asphericity/diopters of achieved defocus correction ratio (the slope of the regression) was  $-0.31$  change in Q-factor (DQ)/D in the CV group and  $-0.47$  DQ/D in the PC group (Fig. 4).

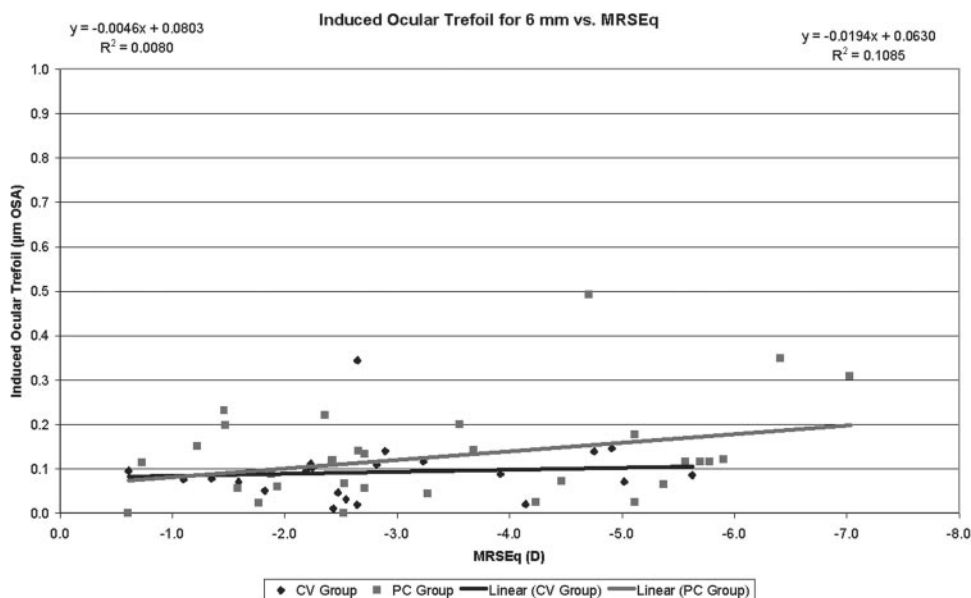


FIGURE 2. Induced ocular trefoil/di-  
opter defocus ratio in the CV and the  
PC groups.

The results of the postoperative evaluation at the 6-month follow-up in both groups are shown in Table 2.

**DISCUSSION**

We designed our centration strategies in two different centration references that can be detected easily and measured with currently available technologies. PC may be the most extensively used centration method for several reasons. First, the pupil boundaries are the standard references observed by the eye-tracking devices. Moreover, the entrance pupil can be well represented by a circular or oval aperture, and these are the most common ablation areas. Centering on the pupil offers the opportunity to minimize the optical zone size. Because in LASIK there is a limited ablation area of approximately 9.25 mm (flap cap), the maximum allowable optical zone will be approximately 7.75 mm. Because laser ablation is a destructive tissue technique, and the amount of tissue removed is directly

related to the ablation area diameter,<sup>29</sup> the ablation diameter, maximum ablation depth, and ablation volume should be minimized. The planned optical zone should be the same size or slightly larger than the functional entrance pupil for the patients' requirements.

The pupil center considered for a patient who fixates properly defines the line-of-sight, which is the reference axis recommended by the OSA<sup>20</sup> for representing the wavefront aberration.

The main HOA effects (main parts of coma and spherical aberrations) arise from edge effects—that is, strong local curvature changes from the optical zone to the transition zone and from the transition zone to the untreated cornea.<sup>30</sup> It then is necessary to emphasize the use of a large optical zone (6.50 mm or more) to cover the scotopic pupil size and a large and smooth transition zone.

Nevertheless, because the pupil center is unstable, a morphologic reference is more advisable. It is well known, more-

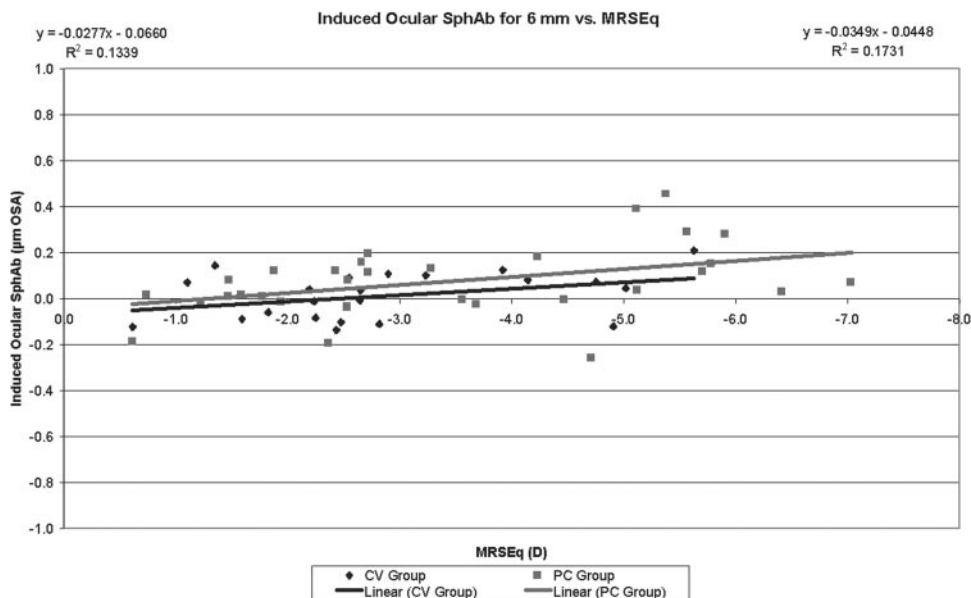


FIGURE 3. Induced spherical ocular  
aberration/di-  
opter defocus ratio in the CV and the PC groups.

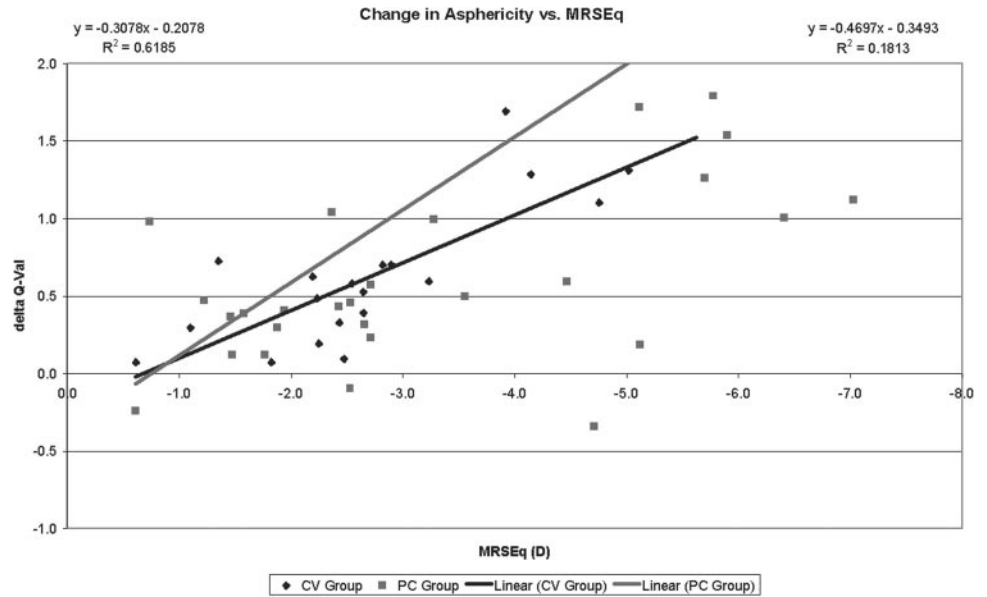


FIGURE 4. Change in asphericity (Q-Value)/defocus diopter ratio in the CV and the PC groups.

over, that the pupil center shifts with changes in pupil size,<sup>31</sup> since the entrance pupil we see is a virtual image of the real one.<sup>32</sup>

The CV in different modalities is the other major choice as the centration reference. In perfectly acquired topography, the CV represents the corneal vertex. In addition, if the human optical system were truly coaxial, the corneal vertex would represent the corneal intercept of the optical axis. Despite the fact that the human optical system is not truly coaxial, the cornea is the main refractive surface. Thus, the corneal vertex represents a stable preferable morphologic reference. However, there are several ways to determine the corneal vertex: the most extensively used one is to determine the coaxial corneal light reflex (first Purkinje image). Nevertheless, as de Ortueta and Arba Mosquera<sup>3</sup> have pointed out, there is a problem in using the coaxial light reflex, because surgeons differ; for instance, the coaxial light reflex is seen differently, depending on the surgeon's eye dominance, the surgeon's eye balance, or the stereopsis angle of the microscope. For example, the LadarVision platform (Alcon) uses a coaxial photograph as reference to determine the coaxial light reflex, which is independent of the surgeon's focus. For that reason, in the present study, ablations were centered using the pupillary offset, the distance between the pupil center and the normal CV, which corresponds to the angle between the line of sight and the optical axis. Thus, the three-dimensional combination

of angle  $\kappa$  minus  $\alpha$  minus  $\lambda$ . The angle  $\kappa$  represents the angle between the pupillary and visual axes, and the angle  $\alpha$  represents the angle between optical and visual axes, angle  $\lambda$  represents the angle between the pupillary axis and the line of sight. Therefore, (visual axis – pupillary axis) – (visual axis – optical axis) – (line-of-sight – pupillary axis) = (optical axis – line of sight; Fig. 5).

In the Figure 5, for practical purposes, the foveola appears too far from the posterior pole and does not correspond to a realistic representation of the eye morphology. However, it helps in understanding the key concept used in our vertex centration approach.

Considering this, for an aberration-free profile, aspherical, or, in general, noncustomized treatments, we use minimal patient data (sphere, cylinder, and axis values) from the diagnosis. Therefore, we assume that the patient's optical system is aberration-free or that those aberrations are not clinically relevant (otherwise, we would have planned a customized treatment). For those reasons, the most appropriate centering reference is the corneal vertex; we then modify the corneal asphericity with an aberration-free ablation profile, including loss of efficiency compensations. For customized wavefront treatments—that is, change in aberrations according to diagnosis measurements—we use a more comprehensive data set from the patient's diagnosis, including the aberrations, because the aberration maps are described for a reference system in the

TABLE 2. Results of Postoperative Evaluations at the 6-Month Follow-up for Both Groups

	CV Group		PC Group	
	Mean ± SD	Range	Mean ± SD	Range
Defocus (D)	-0.26 ± 0.49	-1.25 to +0.75	-0.29 ± 0.40	-1.00 to +0.50
Astigmatism (D)	0.15 ± 0.18	0.00 to 0.50	0.19 ± 0.21	0.00 to 0.50
BSCVA	1.24 ± 0.47	0.8 to 1.4	1.20 ± 0.45	0.7 to 1.4
Ocular coma (μm) (6.0 mm)	0.23 ± 0.11	0.02 to 0.52	0.27 ± 0.17	0.01 to 0.73
Ocular trefoil (μm) (6.0 mm)	0.15 ± 0.09	0.02 to 0.42	0.15 ± 0.08	0.02 to 0.40
Spherical ocular aberration (μm) (6.0 mm)	+0.09 ± 0.29	-0.35 to +0.59	+0.14 ± 0.30	-0.41 to +0.66
RMS HOA (μm) (6.0 mm)	0.48 ± 0.12	0.30 to 0.79	0.51 ± 0.17	0.25 to 0.93
Pupillary offset (mm)	0.28 ± 0.11	0.20 to 0.56	0.30 ± 0.19	0.20 to 0.87

Abbreviation is as in Table 1.

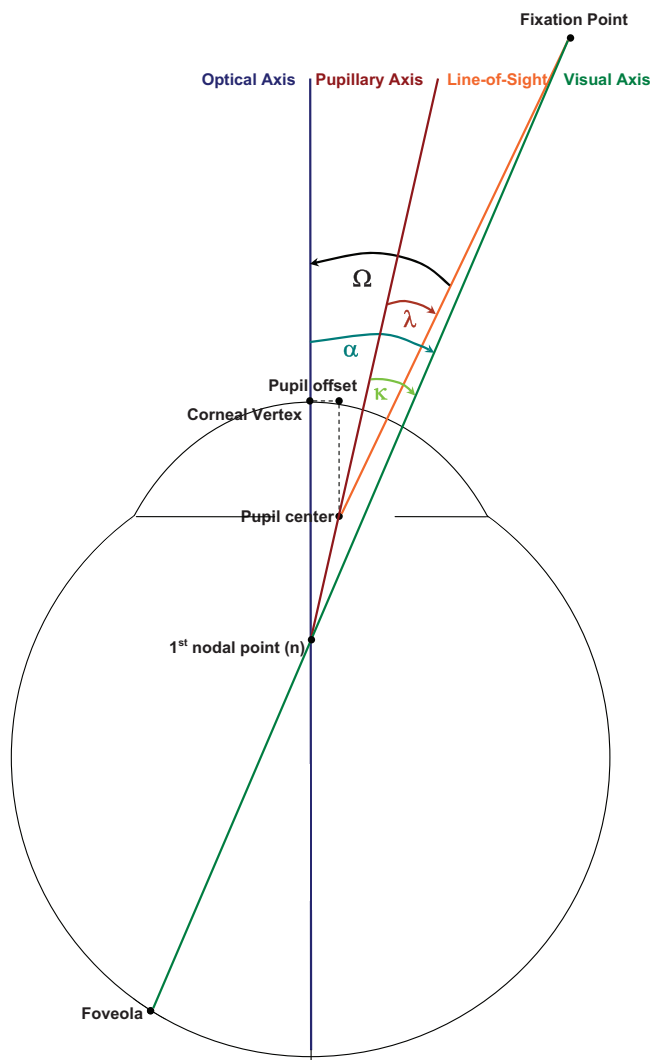


**FIGURE 5.** Diagram showing the key concept of alignment according to the pupillary offset and the relative orientation  $\kappa$  minus  $\alpha$  minus  $\lambda$  angle, which represents the angle between the line of sight and the optical axis.

center of the entrance pupil. The most appropriate centering reference is the entrance pupil, as measured in the diagnosis.<sup>26</sup>

Providing different centering references for different types of treatments is not ideal, because it is difficult to standardize the procedures. Nevertheless, ray tracing indicates that the optical axis is the ideal centering reference. Because this is difficult to standardize and considering that the anterior corneal surface is the main refractive element of the human eye, the CV, defined as the point of maximum elevation, will be the closest reference as proposed here. It shall be, however, noticed that on the less-prevalent oblate corneas the point of maximum curvature (corneal apex) may be off center and not represented by the corneal vertex.

However, it would be interesting to refer the corneal and/or ocular wavefront measurements to the optical axis or the CV. This can be done easily for corneal wavefront analysis, because there is no limitation imposed by the pupil boundaries.<sup>33</sup> However, it is not as easy for ocular wavefront analysis, because the portion of the cornea above the entrance pupil alone is responsible for the foveal vision.<sup>4</sup> Moreover, in patients with corneal problems such as keratoconus/keratectasia, post-LASIK

(pupil-centered), corneal warpage induced by contact lens wearing and other diseases causing irregularity on the anterior corneal surface, the corneal vertex and the corneal apex may shift. In those cases, the pupil center is probably more stable. Moreover, since most laser systems are designed to perform multiple procedures besides LASIK, it is more beneficial that excimer laser systems have the flexibility to choose different centration strategies.

The standard parameters to assess refractive surgery results—that is, efficacy, predictability, refractive outcome, stability, and safety, are inadequate for evaluating the optimal centration reference, at least in patients with myopic astigmatism.

With this analysis, no significant differences have been found that favor any of the centration strategies; however, trends have been found favoring CV treatments for refractive outcome and safety, and PC treatments for efficacy.

Concerning safety, 9% of the eyes lost one line of BSCVA; however, no single eye lost more than one line. The repeatability of the BSCVA within individuals from day to day is approximately one line of BSCVA. Moreover, there was a higher percentage of eyes that gained lines (38% and 24%) than that lost one line (8% and 10%).

A comparison of data in Tables 1 and 2 shows that no evaluated ocular aberration metrics increased in a clinically relevant way with either centration strategy. Further, because the ablation procedures are performed in a physical world, they are always affected by different sources of unavoidable inherent errors<sup>34</sup> that are sources of aberrations,<sup>35</sup> such as biomechanical reactions due to the flap cut,<sup>36,37</sup> blending zones, and cyclotorsion<sup>38</sup> and centration errors, spot size limitations, active eye-tracking<sup>39</sup> capabilities, and biomechanical reactions due to the ablation process.<sup>40</sup>

Although this may indicate that both centration strategies are virtually equivalent, the enrollment was limited to eyes with moderate-to-large pupil offset ( $>200 \mu\text{m}$ ).

A deeper analysis of the induced ocular aberrations and the changes in asphericity showed significant differences favoring CV centration for the induction of coma and spherical ocular aberration and the changes in asphericity and no significant differences for the induced ocular trefoil.

Because of the smaller  $\kappa$  angle associated with myopes compared with hyperopes,<sup>41,42</sup> centration problems are less apparent. However, we wanted to test whether the  $\kappa$  angle in myopes was sufficiently large to show differences in results, because it is always desirable to achieve as much standardization as possible and not to treat the myopes by using one reference, while using another in the hyperopes.

Moreover, no significant differences were found in the pupillary offset before and after the treatments with any centration strategy.

With this analysis, no significant differences in visual outcomes were found that favored either centration strategy, with significant differences occurring only with the ocular aberration and asphericity measurements. The large optical zones used in the present study may be responsible for the lack of difference in postoperative visual outcomes in the two groups. Hyperopic LASIK provides smaller functional optical zones and, for this reason, these results should not be extrapolated to hyperopic LASIK.<sup>11,43</sup>

Previous studies<sup>44</sup> have reported that based on theoretical calculations with 7.0-mm pupils even for customized refractive surgery, that are much more sensitive to centration errors, it appears unlikely that optical quality would be degraded if the lateral alignment error did not exceed 0.45 mm. In 90% of eyes, even an accuracy of 0.8 mm or better would have been sufficient to achieve the goal.<sup>43</sup>

In our case, the pupillary offset averaged 0.29 mm and this moderate value seems to be sufficiently large to be responsible for differences in ocular aberrations, however, not large enough to correlate this difference in ocular aberrations with functional vision.

The accuracy, predictability, and stability of the refractive power change, together with the minimum external impact of the CAM ablation profiles on the HOAs led to superior VAs compared to the preoperative ones in both groups.

A limitation of this study is that we used a comparison based on two different groups of patients, with different centration used as the reference. A direct comparison on a lateral/contralateral eye basis for the assignment of the centration reference may reduce the variability of external uncontrollable effects (such as flap cut, corneal response to the ablation, repeatability of the instruments, and cooperation of the patients). However, such a direct comparison may reduce patients' satisfaction, as patients may after surgery observe differences among eyes due to the different centration.

In summary, the present study showed that morphologic centering references such as the CV, which are not standard in refractive surgery, yielded visual, optical, and refractive results comparable to those of pupil centration techniques for correction of myopia and myopic astigmatism in eyes with moderate to large pupillary offset. No significant differences in the comparative outcomes of both centration strategies were observed in visual results, but they were found in high order aberration results. Despite this, an absolute optimum centration reference could not be determined. Centering on the pupil offers the opportunity to minimize the optical zone size, whereas centering in the CV offers the opportunity to use a stable morphologic axis and to maintain the corneal morphology after treatment. Therefore, centration on the CV has the potential to replace the currently used standard pupil centration to correct noncustomized myopic astigmatism on normal corneas. Further studies are needed to determine stable appropriate centration references.

## References

- Pande M, Hillmann JS. Optical zone centration in keratorefractive surgery: entrance pupil center, visual axis, coaxially sighted corneal reflex, or geometric corneal center? *Ophthalmology*. 1993; 100:1230-1237.
- Boxer Wachler BS, Korn TS, Chandra NS, Michel FK. Decentration of the optical zone: centering on the pupil versus the coaxially sighted corneal light reflex in LASIK for hyperopia. *J Refract Surg*. 2003;19:464-465.
- de Ortueta D, Arba Mosquera S. Centration during hyperopic LASIK using the coaxial light reflex. *J Refract Surg*. 2007;23:11.
- Uozato H, Guyton DL. Centering corneal surgical procedures. *Am J Ophthalmol*. 1987;103:264-275.
- Mandell RB. Apparent pupil displacement in videokeratography. *CLAO J*. 1994;20:123-127.
- Munnerlyn CR, Koons SJ, Marshall J. Photorefractive keratectomy: a technique for laser refractive surgery. *J Cataract Refract Surg*. 1988;14:46-52.
- Mastropasqua L, Toto L, Zuppari E, et al. Photorefractive keratectomy with aspheric profile of ablation versus conventional photorefractive keratectomy for myopia correction: six-month controlled clinical trial. *J Cataract Refract Surg*. 2006;32:109-116.
- Mrochen M, Jankov M, Bueeler M, Seiler T. Correlation between corneal and total wavefront aberrations in myopic eyes. *J Refract Surg*. 2003;19:104-112.
- Alio JL, Belda JJ, Osman AA, Shalaby AM. Topography-guided laser in situ keratomileusis (TOPOLINK) to correct irregular astigmatism after previous refractive surgery. *J Refract Surg*. 2003;19:516-527.
- Mrochen M, Kaemmerer M, Seiler T. Clinical results of wavefront-guided laser in situ keratomileusis 3 months after surgery. *J Cataract Refract Surg*. 2001;27:201-207.
- Mrochen M, Donetzky C, Wüllner C, Löffler J. Wavefront-optimized ablation profiles: theoretical background. *J Cataract Refract Surg*. 2004;30:775-785.
- Koller T, Iseli HP, Hafezi F, et al. Q-factor customized ablation profile for the correction of myopic astigmatism. *J Cataract Refract Surg*. 2006;32:584-589.
- Levy Y, Segal O, Avni I, Zadok D. Ocular higher-order aberrations in eyes with supernormal vision. *Am J Ophthalmol*. 2005;139: 225-228.
- Pablo Artal. *What Aberration Pattern (If Any) Produces the Best Vision?* Presented at the Sixth International Wavefront Congress, Athens, Greece; February 2005.
- Marcos S, Cano D, Barbero S. Increase in corneal asphericity after standard laser in situ keratomileusis for myopia is not inherent to the Munnerlyn algorithm. *J Refract Surg*. 2003;19:S592-S596.
- Dorronsoro C, Cano D, Merayo-Llodes J, Marcos S. Experiments on PMMA models to predict the impact of corneal refractive surgery on corneal shape. *Opt Express*. 2006;14:6142-6156.
- Arba Mosquera S, de Ortueta D. Geometrical analysis of the loss of ablation efficiency at non-normal incidence. *Opt Express*. 2008;16: 3877-3895.
- Thibos LN. *Wavefront Data Reporting and Terminology*. Presented at the Second International Wavefront Congress, Monterey, CA, February 2001.
- Thibos L, Bradley A, Applegate R. Accuracy and precision of objective refraction from wavefront aberrations. *Invest Ophthalmol Vis Sci*. 2004;44(4):329-351.
- de Ortueta D. Planar flaps with the Carriazo-Pendular microkeratome. *J Refract Surg*. 2008;24(4):322; author reply 322-323.
- de Ortueta D, Arba-Mosquera S. Topographical changes after hyperopic LASIK with the ESIRIS laser platform. *J Refract Surg*. 2008;24:137-144.
- Huang D, Arif M. Spot size and quality of scanning laser correction of higher-order wavefront aberrations. *J Cataract Refract Surg*. 2002;28:407-416.
- Guirao A, Williams D, MacRae S. Effect of beam size on the expected benefit of customized laser refractive surgery. *J Refract Surg*. 2003;19:15-23.
- Bende T, Seiler T, Wollensak J. Side effects in excimer corneal surgery. Corneal thermal gradients. *Graefes Arch Clin Exp Ophthalmol*. 1988;226:277-280.
- Bueeler M, Mrochen M. Simulation of eye-tracker latency, spot size, and ablation pulse depth on the correction of higher order wavefront aberrations with scanning spot laser systems. *J Refract Surg*. 2005;21:28-36.
- Zernike F. Diffraction theory of the knife-edge test and its improved form, the phase-contrast method. *Monthly Notices of the Royal Astronomical Society*. 1934;94:377-384.
- Thibos LN, Applegate RA, Schwiegerling JT, Webb R; VSIA Standards Taskforce Members. Standards for reporting the optical aberrations of eyes. *J Refract Surg*. 2002;18:S652-S660.
- Guirao A, Williams D, Cox I. Effect of rotation and translation on the expected benefit of an ideal method to correct the eyes higher-order aberrations. *J Opt Soc Am A*. 2001;18:1003-1015.
- Gatinel D, Hoang-Xuan T, Azar DT. Determination of corneal asphericity after myopia surgery with the excimer laser: a mathematical model. *Invest Ophthalmol Vis Sci*. 2001;42:1736-1742.
- Marcos S, Barbero S, Llorente L, Merayo-Llodes J. Optical response to LASIK surgery for myopia from total and corneal aberration measurements. *Invest Ophthalmol Vis Sci*. 2001;42:3349-3356.
- Yang Y, Thompson K, Burns S. Pupil location under mesopic, photopic and pharmacologically dilated conditions. *Invest Ophthalmol Vis Sci*. 2002;43:2508-2512.
- Schruender S, Fuchs H, Spasovski S, Dankert A. Intraoperative corneal topography for image registration. *J Refract Surg*. 2002; 18:S624-S629.

33. Salmon TO. *Corneal Contribution to the Wavefront Aberration of the Eye*. PhD Thesis. Bloomington, IN: Indiana University; 1999: 70.
34. Lipshitz I. Thirty-four challenges to meet before excimer laser technology can achieve super vision. *J Refract Surg*. 2002;18:740-743.
35. Marcos S. Aberrations and visual performance following standard laser vision correction. *J Refract Surg*. 2001;17:S596-S601.
36. Tran DB, Sarayba MA, Bor Z, et al. Randomized prospective clinical study comparing induced aberrations with IntraLase and Hansatome flap creation in fellow eyes. *J Cataract Refract Surg*. 2005;31:97-105.
37. Durrie DS, Kezirian GM. Femtosecond laser versus mechanical keratome flaps in wavefront-guided laser in situ keratomileusis. *J Cataract Refract Surg*. 2005;31:120-126.
38. Smith EM Jr, Talamo JH. Cyclotorsion in the seated and the supine patient. *J Cataract Refract Surg*. 1995;21:402-403.
39. Tsai YY, Lin JM. Ablation centration after active eye-tracker-assisted photorefractive keratectomy and laser in situ keratomileusis. *J Cataract Refract Surg*. 2000;26:28-34.
40. Yoon G, MacRae S, Williams DR, Cox IG. Causes of spherical aberration induced by laser refractive surgery. *J Cataract Refract Surg*. 2005;31:127-135.
41. Artal P, Benito A, Tabernero J. The human eye is an example of robust optical design. *J Vision*. 2006;6:1-7.
42. Tabernero J, Benito A, Alcón E, Artal P. Mechanism of compensation of aberrations in the human eye. *J Opt Soc Am A*. 2007;24:3274-3283.
43. Llorente L, Barbero S, Merayo J, Marcos S. Changes in corneal and total aberrations induced by LASIK surgery for hyperopia. *J Refract Surg*. 2004;20:203-216.
44. Bueeler M, Mrochen M, Seiler T. Maximum permissible lateral decentration in aberration-sensing and wavefront-guided corneal ablations. *J Cataract Refract Surg*. 2003;29:257-263.